

# PCCP

Accepted Manuscript



This is an *Accepted Manuscript*, which has been through the Royal Society of Chemistry peer review process and has been accepted for publication.

*Accepted Manuscripts* are published online shortly after acceptance, before technical editing, formatting and proof reading. Using this free service, authors can make their results available to the community, in citable form, before we publish the edited article. We will replace this *Accepted Manuscript* with the edited and formatted *Advance Article* as soon as it is available.

You can find more information about *Accepted Manuscripts* in the [Information for Authors](#).

Please note that technical editing may introduce minor changes to the text and/or graphics, which may alter content. The journal's standard [Terms & Conditions](#) and the [Ethical guidelines](#) still apply. In no event shall the Royal Society of Chemistry be held responsible for any errors or omissions in this *Accepted Manuscript* or any consequences arising from the use of any information it contains.

## A Co(II)-Ru(II) dyad relevant to light-driven water oxidation catalysis.

Cite this: DOI: 10.1039/x0xx00000x

Alejandro Montellano López,<sup>a\*</sup> Mirco Natali,<sup>b\*</sup> Erica Pizzolato,<sup>a</sup> Claudio Chiorboli,<sup>c</sup> Marcella Bonchio,<sup>a</sup> Andrea Sartorel<sup>\*a</sup> and Franco Scandola<sup>\*b</sup>

Received 00th January 2012,

Accepted 00th January 2012

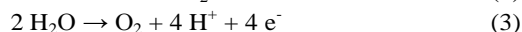
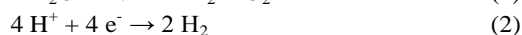
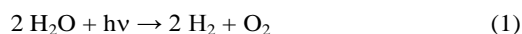
DOI: 10.1039/x0xx00000x

www.rsc.org/

Artificial photosynthesis aims at efficient water splitting into hydrogen and oxygen, by exploiting solar light. As a priority requirement, this process entails the integration of suitable multi-electron catalysts with light absorbing units, where charge separation is generated in order to drive the catalytic routines. The final goal could be the transposition of such asset into a photoelectrocatalytic cell, where the two half-reactions, proton reduction to hydrogen and water oxidation to oxygen, take place at two properly engineered photoelectrodes. We herein report a covalent approach to anchor a Co(II) water oxidation catalyst to a Ru(II) polypyridine photosensitizer unit; photophysical characterisation and catalytic activity of such dyad in a light activated cycle are reported, and implications for the development of regenerative systems are discussed.

### Introduction

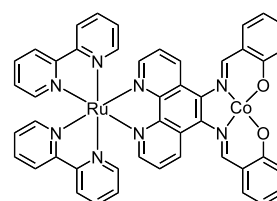
The main goal of artificial photosynthesis is the use of solar light for water splitting, to yield hydrogen as a clean and renewable fuel (eq. 1).<sup>1</sup> A general operating scheme foresees a light-induced charge separation centre, that drives the redox events involved in the overall process: reduction of protons to hydrogen, and oxidation of water to oxygen (eqs. 1-3).<sup>2</sup>



In particular, water oxidation to oxygen is a  $4 \text{e}^- / 4 \text{H}^+$  process where a new O-O bond is formed, and is therefore recognized as a transformation with complex mechanistic aspects that suffer from high kinetic barriers.<sup>3</sup> In recent years, formidable efforts have been dedicated to the development of new catalysts for water oxidation (water oxidation catalysts, WOC), with particular emphasis on light activated conditions.<sup>4</sup> These are usually performed in a homogeneous model system, combining the catalyst with a suitable photosensitizer (i.e. Ru(bpy)<sub>3</sub><sup>2+</sup>, bpy = 2,2'-bipyridine) and a sacrificial electron acceptor (i.e. sodium persulfate, Na<sub>2</sub>S<sub>2</sub>O<sub>8</sub>);<sup>5</sup> the ultimate perspective is however the development of regenerative systems, where the catalyst and the photosensitizer are anchored onto a semiconductor surface, in the photoanode compartment of a regenerative photoelectrocatalytic cell.<sup>6</sup> In such operating scheme, the electron transfer rate from the WOC to the photosensitizer has a marked impact on the performance

and stability of the overall system,<sup>6,7</sup> in particular to prevent side reactions leading to photosensitizer self-oxidation and degradation, or to unproductive charge recombination.<sup>6,7</sup> Therefore, in order to boost such electron transfer rate, several approaches have been proposed to enhance WOC-photosensitizer interactions, including covalent linkages or supramolecular assemblies.<sup>8</sup>

Photosensitizer moiety



Catalyst moiety

Fig. 1 Representation of the covalent dyad 1.

In this paper, we present the synthesis, electrochemical and photophysical characterization of a novel WOC-photosensitizer dyad **1**, based on a compartmental Co(II)-Ru(II) covalent assembly (figure 1). The catalytic moiety is based on a single site Co(II)-salophen unit, that we have recently reported as capable of catalysing water oxidation in a light activated cycle.<sup>9</sup> Its covalent linkage to a Ru<sup>II</sup>(bpy)<sub>2</sub> photosensitizer moiety is obtained by a suitable functionalization of a phenanthroline type ligand. Combined electrochemical and photophysical studies reveal that photoinduced, intramolecular redox events involving the two metal centres occur within a very short timescale, confirming efficient electronic interactions between the two

units. Moreover, a preliminary study dealing with activity of **1** in light driven water oxidation is presented, and perspectives towards the application of dyads of such type to regenerative photoanodes are discussed.

## Results and Discussion

### Synthesis and electrochemical characterisation

Synthesis of the compartmental dyad **1** (fig. 2) was accomplished adapting a literature procedure for a Ruthenium-Copper analog reported by Pellegrin *et al.*<sup>10</sup>

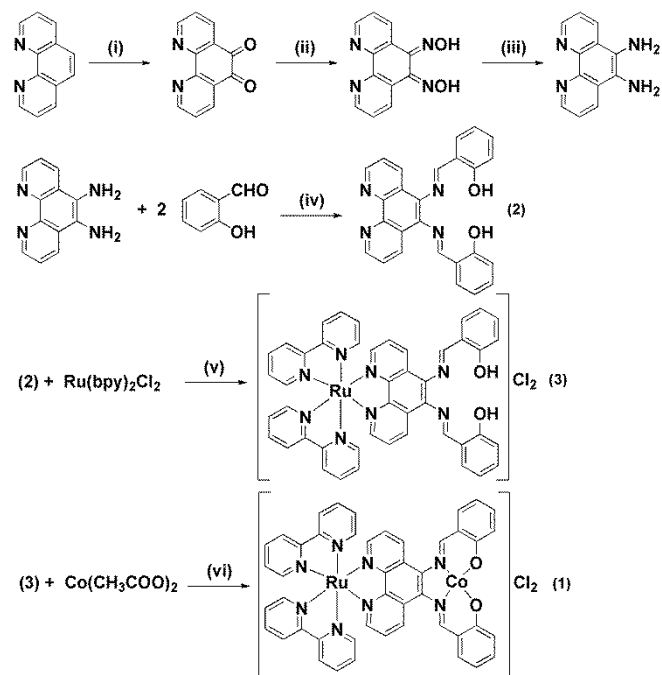


**Fig. 2** Synthesis of **1**. (i)  $\text{H}_2\text{SO}_4/\text{HNO}_3$ , NaBr,  $100^\circ\text{C}$ , yield 35%; (ii)  $\text{NH}_2\text{OH}\cdot\text{HCl}$ ,  $\text{BaCO}_3$  in refluxing ethanol, yield 57%; (iii) 10% Pd/C,  $\text{N}_2\text{H}_4$  in refluxing ethanol, yield 42%; (iv) triethylorthoformate in refluxing ethanol, yield 42%; (v) triethylorthoformate,  $\text{AgNO}_3$  in refluxing ethanol, yield 66%; (vi) methanol, room temperature, yield 91%.

The key intermediate is the heteroditopic ligand *N,N'*-bis(salicylidene)-5,6-(1,10-phenanthroline)diamine, **2**, prepared by a four-step synthesis starting from 1,10-phenanthroline. These steps include: (i) oxidation of 1,10-phenanthroline to 1,10-phenanthroline-5,6-dione under reflux of  $\text{H}_2\text{SO}_4/\text{HNO}_3$ ,<sup>11a</sup> (ii) reaction with hydroxylamine to yield the 1,10-phenanthroline-5,6-dioxime,<sup>11b</sup> (iii) its reduction to 1,10-phenanthroline-5,6-diamine with hydrazine,<sup>11b</sup> and (iv) condensation of 1,10-phenanthroline-5,6-diamine with two equivalents of salicylaldehyde.<sup>10</sup> The identity of all intermediates was confirmed by comparison of ESI-MS, infrared and  $^1\text{H-NMR}$  characterisation with literature (see figure S1 in ESI for  $^1\text{H-NMR}$  of **2**). Metallation of the phenanthroline unit with Ru(II) was then achieved by reaction of **2** with *cis*- $\text{Ru}(\text{bpy})_2\text{Cl}_2$ , under refluxing methanol in the presence of triethylorthoformate;<sup>10</sup> in the resulting complex, **3**, isolated in 66% yield, the Ru(II) centre is coordinated to the heteroditopic ligand **2**, while maintaining the two bpy ligands in its coordination sphere, as confirmed by elemental analysis and by  $^1\text{H-NMR}$

characterisation (figure S2 in ESI). The final step is metallation of the salophen cavity with Co(II), readily achieved under room temperature conditions by addition of Cobalt acetate to a methanol solution of **3**, precipitating the product **1** in 91% yield by addition of diethyl ether.

Electrochemical characterization of dyad **1** and of the Cobalt free analog **3** were initially performed in acetonitrile solution (figure 3 and table 1).

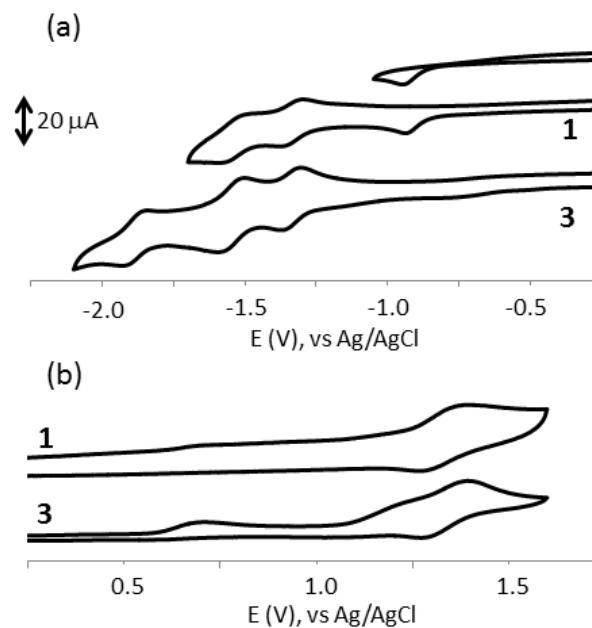


**Fig. 3** Cyclic voltammograms of **1** and **3** under cathodic (a) and anodic (b) scans. 0.5 mM in acetonitrile, 0.1 M tetra-*n*-butylammonium perchlorate as supporting electrolyte. Working electrode glassy carbon, counter electrode: platinum wire, reference electrode: Ag/AgCl (3 M NaCl).

Under cathodic scan, **3** shows three reversible reduction waves at  $E_{1/2} = -1.34, -1.54$  and  $-1.89$  V vs Ag/AgCl (figure 4a and table 1). These are consistent with subsequent one-electron reductions at the phenanthroline based and bpy ligands.<sup>10,12</sup> The first two reduction events are observed also for **1**, at almost unaffected potentials; moreover, an irreversible process is observed at  $-0.94$  V, and ascribed to the reduction of Co(II) to Co(I) coordinated by a salophen ligand.<sup>13</sup>

**Table 1.** Potentials associated to redox processes of **1** and **3** in acetonitrile solution.

	E (V), vs Ag/AgCl					
<b>1</b>	-1.54	-1.34	-0.94 <sup>a</sup>			1.32
<b>3</b>	-1.89	-1.54	-1.34	0.70 <sup>b</sup>	1.23 <sup>b</sup>	1.33

<sup>a</sup> cathodic peak for irreversible process; <sup>b</sup> anodic peak for irreversible process.

Under anodic scan, two irreversible processes are observed for **3** at 0.70 and 1.23 V, compatible with oxidation at the salophen moiety, likely involving the phenol groups.<sup>10</sup> A third, reversible event at  $E_{1/2} = 1.33$  V is observed, and attributed to the  $\text{Ru}^{\text{III/II}}$  couple. In the case of **1**, only the reversible wave due to  $\text{Ru}^{\text{III/II}}$  couple is observed at  $E_{1/2} = 1.32$  V, since the hydroxo

groups of the salophen moiety are involved in the coordination of the Cobalt centre and therefore protected from oxidation.♣

### Photophysical characterisation in acetonitrile

Absorption spectra of **1** and **3** in acetonitrile are reported in figure 4, compared to Ru(bpy)<sub>3</sub><sup>2+</sup>. In both cases, a metal-to-ligand charge transfer (MLCT) band centered at 460 nm is observed, typical of ruthenium polypyridine sensitizers. In the case of **1**, a second broad absorption between 350-450 nm superimposes which may be attributed to Cobalt based transitions.<sup>9,14</sup> Finally, ligand-centered (LC) transitions in the 250-350 nm region can also be discerned ascribable to the 2,2'-bipyridine (maximum at 288 nm) and to the phenantroline-based (maxima at 334 and 348 nm) units.<sup>10,15</sup>

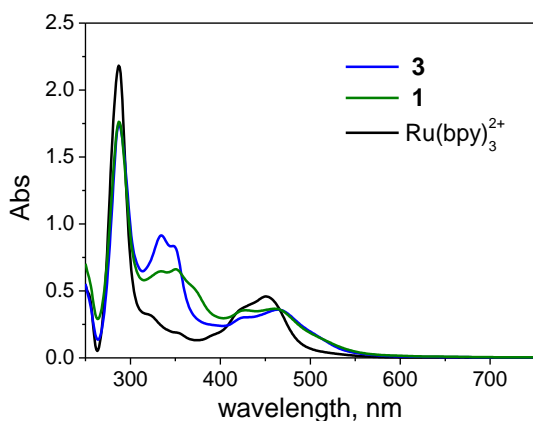


Fig. 4 Absorption spectra in acetonitrile of molecular dyads **1**, **3**, and model Ru(bpy)<sub>3</sub><sup>2+</sup>.

Upon excitation at 466 nm, the emission of both **1** and **3** in acetonitrile solution is almost completely quenched (>95% with respect to a solution of Ru(bpy)<sub>3</sub><sup>2+</sup> with the same optical density). Analysis of the transient absorption spectra obtained by Ultrafast Spectroscopy (UFS) allows to dissect the electron transfer events responsible for the abatement of the emission (figures 5 and 6). In the case of **3** (figure 5), the initial transient spectrum (1 ps time delay), featuring the MLCT bleach and a broad absorption at longer wavelength with a relative maximum at 530 nm, can be reasonably assigned to the triplet excited state, promptly formed after 400-nm excitation by ultrafast intersystem crossing from the singlet excited state. The subsequent spectral changes are clearly biphasic. In the time window between 1-244 ps (figure 5a) the MLCT bleach practically disappears, while the positive absorption increases in intensity with a shift of the maximum from 530 nm to 510 nm; the time constant for this first process is ca. 45 ps (figure S3 in ESI). Then, this new transient starts decaying to the baseline in the time interval between 244-1890 ps (figure 5b). The time resolution of the experiment (2000 ps) does not allow any reliable detection of the kinetic parameter for this second process. However, the same transient spectrum can be revealed also by laser flash photolysis with a time profile following that of the excitation source (6-8 ns, figure S4 of ESI). This means that the transient produced in the first hundred ps, as observed

by UFS, decays to the ground state with a time constant of about 6-8 ns.

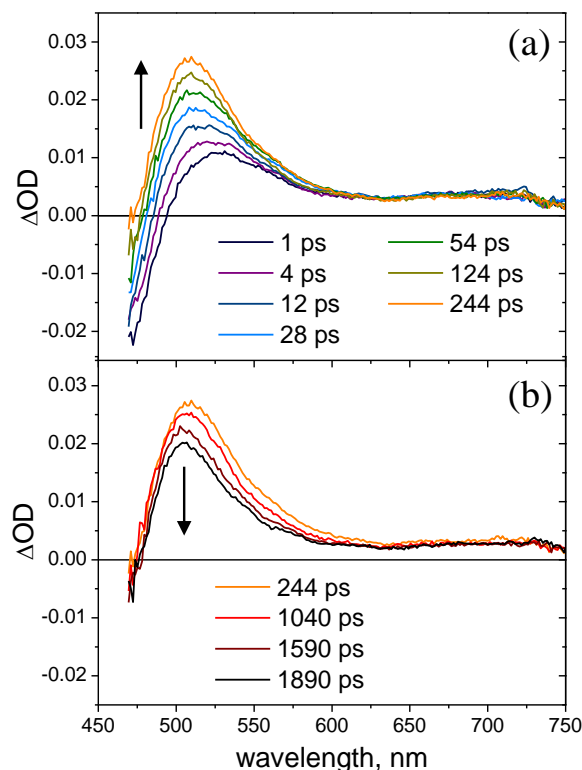


Fig. 5 Difference absorption spectra at (a) 1-244 ps and (b) 244-1890 ps time delays obtained by UFS (400-nm excitation) on **3** in acetonitrile.

According to the electrochemical data, only reductive quenching of the MLCT excited state is thermodynamically allowed (with a driving force of ca. -0.2 eV, without electrostatic correction applied), with reduction of the bipyridyl ligand of the complex and oxidation of the aromatic hydroxy groups of the salophen moiety. As a matter of fact, formation of a positive absorption with a maximum at 510 nm is a fingerprint<sup>16</sup> of the reduction of ruthenium polypyridine complexes.\*\* This proton-coupled process is likely assisted by intramolecular hydrogen bonding within the Schiff base moiety of the ligand.<sup>17</sup>

When the Cobalt centre is inserted within the salophen cavity, the photophysical processes change sensitively. Similarly to **3**, the prompt transient spectrum obtained by UFS corresponds to the triplet MLCT excited state. In this case (figure 6a), however, the positive absorption at 530 nm decays rapidly with a time constant of 15 ps (figure S5). In this process (isosbestic point at 485 nm and  $\Delta OD = -0.005$ ), a long-lived transient is formed, characterized by little positive absorption and substantial bleach left at 470 nm. This transient decays (figure 6b) with recovery of the 470-nm bleach in a much longer time scale (estimated lifetime ca. 6 ns, figure S5). Overall, these spectral changes are compatible† with fast oxidative quenching of the MLCT excited state by the cobalt center, followed by slow charge recombination.

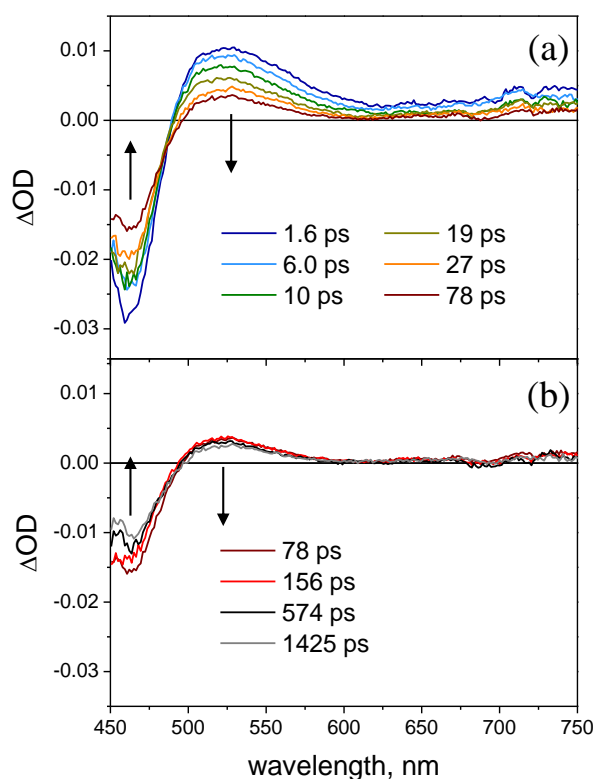


Fig. 6 Difference absorption spectra at (a) 1-78 ps and (b) 78-1425 ps time delays obtained by UFS (400-nm excitation) on **1** in acetonitrile.

### Photophysical characterisation in aqueous buffer and light driven water oxidation

The behaviour of **1** and **3** has been examined also in aqueous solutions, as the target solvent for artificial photosynthesis. The photophysical properties of **1** and **3** change dramatically in aqueous phosphate buffer at pH 7, where partial recovery of the typical emission of Ru(II) polypyridine species is observed for both compounds (figure 7a). Moreover, the static nature of the quenching, as observed from the time-resolved decay of the MLCT emission (figure 7b) strongly suggests that the aqueous environment introduces new chemical equilibria affecting the photoinduced dynamics. In the case of **3**, partial protonation of the salophenic ligand may take place in phosphate buffer at pH 7, thus preventing the proton-coupled electron transfer mechanism of the reductive quenching.<sup>§</sup>

Concerning compound **1**, the lack of quenching by the Co centre seems to be hardly attributable to a simple solvent effect. A possible explanation could be the presence of more complex equilibria in aqueous environment, possibly involving (i) coordination of axial ligands<sup>18</sup> making oxidative quenching thermodynamically unfavourable or, more likely, (ii) partial leaching of cobalt. This could be relevant to the evaluation of light activated water oxidation.

Light activated water oxidation catalytic tests with **1** were conducted in solution, in the presence of 5 mM sodium persulfate ( $\text{Na}_2\text{S}_2\text{O}_8$ ) as the sacrificial electron acceptor, and of 1 mM  $\text{Ru}(\text{bpy})_3^{2+}$  as photosensitizer.<sup>80</sup>

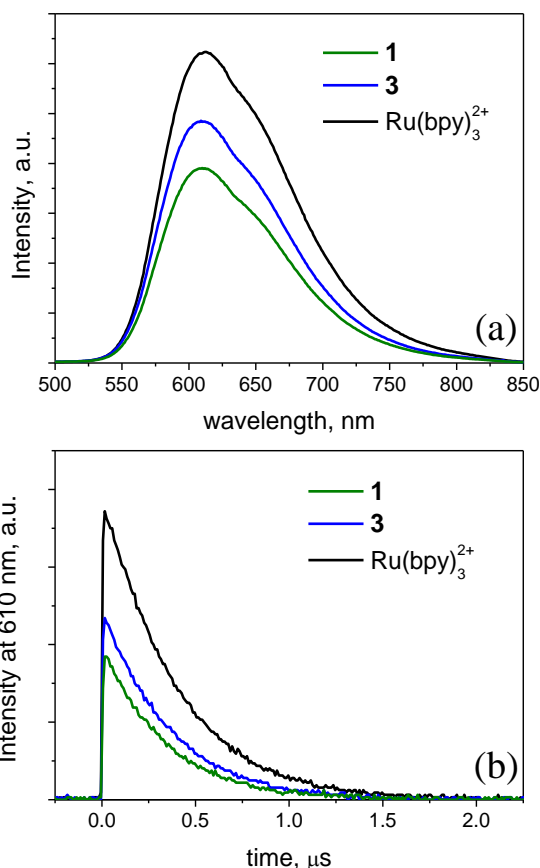
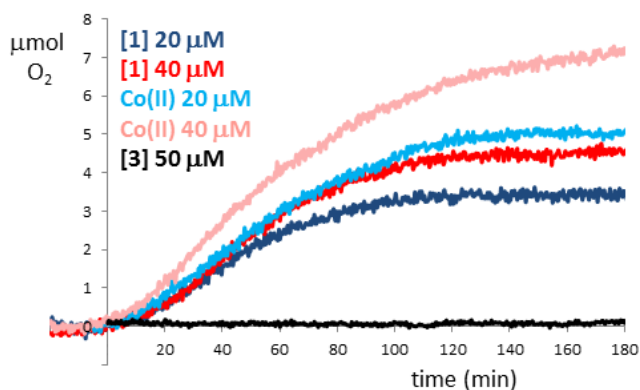


Fig. 7 (a) Photoluminescence spectra (excitation at 400 nm, optically matched solutions) and (b) emission intensity at 610 nm observed by laser flash photolysis (excitation at 355 nm, optically matched solutions) in 20 mM phosphate buffer (pH 7) of **1**, **3**, and  $\text{Ru}(\text{bpy})_3^{2+}$ .

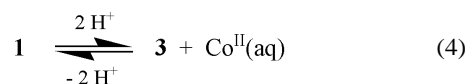
In figure 8, kinetics of  $\text{O}_2$  evolution with 20 and 40  $\mu\text{M}$  of **1** are reported (blue and red traces, respectively). In these two runs, 3.50 and 4.55  $\mu\text{mol}$  of  $\text{O}_2$  are produced after 3 hours; these correspond to a total turnover number per Cobalt center of 11.7 and 7.6, respectively. The maximum  $\text{O}_2$  production rates (measured in the linear range of the kinetic profile, between 5 and 10 minutes after irradiation) are  $0.80$  and  $0.96 \times 10^{-4} \mu\text{mol}(\text{O}_2)\text{s}^{-1}$ , corresponding to turnover frequencies of 2.67 and  $1.61 \times 10^{-3} \text{ s}^{-1}$ , respectively. The quantum yield ( $\Phi$ ) of the process for the reaction where  $[\mathbf{1}] = 40 \mu\text{M}$ , defined as the ratio between the rate of  $\text{O}_2$  produced and the photon flux absorbed by the system,<sup>3c</sup> is 0.037. Since the maximum value of the quantum yield in sacrificial cycles using sodium persulfate is 0.5, this value corresponds to overall 7.4% quantum efficiency of the system.<sup>3c</sup> As expected, the cobalt free system **3** is inactive under the same reaction conditions (black trace in figure 8).

In order to check if the catalytic activity could be partially ascribed to Co(II) ions leaching from **1** (hypothesis (ii) presented above),<sup>19</sup> oxygen evolution tests were run also with  $\text{Co}(\text{NO}_3)_2$  as the catalyst, at the same metal concentrations (light blue and pink traces in figure 8).



**Fig. 8** Kinetics of O<sub>2</sub> evolution from 15 ml of 20 mM phosphate buffer, pH 7 with 5 mM Na<sub>2</sub>S<sub>2</sub>O<sub>8</sub>, 1 mM Ru(bpy)<sub>3</sub><sup>2+</sup> illumination by 1 LED emitting at 450 nm (photon flux 2.63×10<sup>-8</sup> einstein/s). Blue trace: 20 μM **1**; red trace: 40 μM **1**; light blue trace: 20 μM Co(NO<sub>3</sub>)<sub>2</sub>; pink trace: 40 μM Co(NO<sub>3</sub>)<sub>2</sub>; black trace: 50 μM **3**.

Oxygen evolution occurs in the presence of either **1** or Co(II) ions as catalyst, with similar kinetic profiles in the concentration range 20–40 μM (figure 8). Therefore, the presence of dissociation equilibria generating Co(II) aquo-ions from **1** (eq. 4) cannot be ruled out by kinetic evidence.¶ This equilibria hypothesis can justify the partial emission recovery observed when **1** is dissolved in aqueous solution as compared to the quenched system in acetonitrile. The emission properties can thus be ascribed to ligand **3**, generated from **1** upon partial leaching of Co(II) centre (figure 7, see above discussion). Therefore, under the conditions explored, oxygen evolving catalysis is likely due to both **1** and aquo Co(II) ions in 20:80 ratio as possibly estimated by the emission intensity in figure 7.♦



In photocatalytic cycles of this kind<sup>6b,7e-h,9</sup> the primary process is the oxidative quenching of the sensitizer MLCT excited state by S<sub>2</sub>O<sub>8</sub><sup>2-</sup>, with generation of a Ru(III) species, followed by hole transfer to the catalyst. Flash photolysis experiments have been performed to probe the photoinduced generation of Ru(III) by excitation of **1** or **3** (50 μM, λ<sub>exc</sub>=355 nm), with 5 mM Na<sub>2</sub>S<sub>2</sub>O<sub>8</sub> in phosphate buffer (pH 7). With ligand **3**, after a few nanoseconds (time resolution given by the laser pulse) very little amounts of Ru(III) is detected, ca. 5% of what expected from comparative experiments carried out with Ru(bpy)<sub>3</sub><sup>2+</sup> (Figure S7a,c). This result is very likely ascribable to fast (sub-ns)<sup>o</sup> intramolecular hole scavenging from Ru(III) by the phenolic moieties. The fact that a similar, very small amount of Ru(III) is obtained with dyad **1** (Figure S7b) is fully consistent with the hypothesis of extensive (ca 80%) dissociation of **1** to **3**.

## Conclusions

In this paper, we have presented a novel covalent dyad **1**, based on a compartmental Co(II)-Ru(II) assembly, where a Cobalt(II)-salophen unit (water oxidation catalytic moiety) is anchored to a Ru(II) unit with bipyridine and phenanthroline type ligands (photosensitizer moiety). The photophysical characterization of **1** in acetonitrile solution reveals that light absorption by the photosensitizer moiety produces a triplet MLCT excited state, with a lifetime of 15 ps; this very short value is attributed to oxidative quenching of the photosensitizer moiety by the Co(II) ion. In principle, this type of fast quenching of the sensitizer might be detrimental to the use of **1** in photocatalytic water oxidation systems, in particular in homogeneous systems taking advantage of persulfate as a sacrificial electron acceptor, where oxidative quenching of the photosensitizer excited state occurs via a bimolecular route, in a typical timescale of tens of ns.<sup>3a,4c,6b,7e-h,9</sup> It should be remarked, however, that in regenerative systems where the sensitizer-catalyst dyad is supported onto a surface of a semiconductor,<sup>6d,e</sup> electron injection into the conduction band of the semiconductor is usually very fast, as it can occur in hundreds fs.<sup>20</sup> Therefore, a sensitizer/catalyst dyad displaying intramolecular quenching could still be considered for such applications.

A second aspect that has to be considered is stability of the dyad in aqueous environment. The photophysical characterisation of **1** in phosphate buffer, and its catalytic activity within a Ru(bpy)<sub>3</sub><sup>2+</sup>/S<sub>2</sub>O<sub>8</sub><sup>2-</sup> photocatalytic system, suggest instability of **1**, likely due to partial leaching of the cobalt centre. It is worth mentioning that, in this respect, the behaviour of **1** is markedly different from that observed for the Cobalt(II) complex with the salophen ligand (N,N'-bis(salicylaldehyde)-1,2-phenyldiamine), that was found to be stable in aqueous buffer.<sup>9</sup> The reasons for this difference are not obvious. They might be related to the cationic character of **1**, and to the enhanced electron-withdrawing character of the salophen moiety in **1**, with destabilisation of the coordination of cobalt ion, especially in its low oxidation state. More importantly, the steric hindrance between the protons in 4 and 4' positions of the phenanthroline moiety and the protons of the imine groups, are expected to cause a slight distortion of the salophenic ligand,<sup>10a</sup> thereby determining instability towards Cobalt coordination. In any case, strategies to reinforce the stability towards aqueous environment should be considered, in order to propose salophen-based dyads for the design of efficient and durable photoanodes.

## Experimental part

### Synthesis

**Synthesis of 1,10-phenanthroline-5,6-dione.** 1,10-phenanthroline-5,6-dione was synthesized following the procedure described by Yamada *et al.*<sup>11a</sup> A 250 mL round bottom flask containing 4g (22.2 mmol) of 1,10-phenanthroline monohydrate and 24 g (201.6 mmol) of potassium bromide was cooled to 0 °C using an ice bath. Concentrated sulphuric acid

(80 mL) was added in small portions followed by concentrated nitric acid (40 mL). The resulting solution was heated for 2 h at 100°C, cooled to room temperature and poured into 500 mL of water. The solution was neutralized using a 0.1 M sodium hydroxide solution and extracted with dichloromethane. The organic phases were collected and the solvent was evaporated to yield 1.5 g of a yellow solid (35% yield). Characterisation was in agreement with literature data.<sup>11a</sup>

**Synthesis of 1,10-phenanthroline-5,6-dioxime.** 1,10-phenanthroline-5,6-dioxime was synthesized following the procedure described by Bodige *et al.*<sup>11b</sup> A dispersion containing a mixture of 1.5 g (7.2 mmol) of 1,10-phenanthroline-5, 6-dione, 1.82 g (9.2 mmol) in 150 mL of ethanol were stirred and refluxed for 12 hours. The solvent was evaporated under reduced pressure and treated with 140 mL of 0.2 M NH<sub>2</sub>OH·HCl, stirred for 30 minutes and filtered. The light yellowish solid was thus washed with small fractions of water, ethanol and diethyl ether, and dried under vacuum to yield 1 g (57% yield). Characterisation was in agreement with literature data.<sup>11b</sup>

**Synthesis of 1,10-phenanthroline-5,6-diamine.** 1,10-phenanthroline-5,6-diamine was synthesized following the procedure described by Bodige *et al.*<sup>11b</sup> A dispersion of 820 mg (3.34 mmol) of 1,10-phenanthroline-5, 6-dioxime and 800 mg of Pd-C (10%) in 100 mL of absolute ethanol was purged with N<sub>2</sub> for 15 min and heated to reflux. To this mixture, a solution of 7.5 mL of hydrazine monohydrate and 30 mL of ethanol was added over a period of one hour and the resulting mixture refluxed for 12 hours. The mixture was filtered hot through a bed of Celite and the pad was washed several times with 20 mL each of boiling ethanol. The filtrate was taken to dryness and the residue was triturated with 45 mL of water and left at 4 °C overnight. The tan precipitate was filtered and washed with cold water to obtain 300 mg of the desired product (42% yield). Characterisation was in agreement with literature data.<sup>11b</sup>

**Synthesis of (2).** *N,N'*-bis(salicylidene)-5,6-(1,10-phenanthroline)diamine, **2**, was synthesized adapting the procedure described by Pellegrin *et al.*<sup>10</sup> In a round bottom flask, 200 mg (0.95 mmol) of 1,10-phenanthroline-5,6-diamine and 2 mL (20 mmol) of salicylaldehyde were suspended in absolute ethanol together with some drops of triethylorthoformate. The mixture was heated to reflux for 3 hours to observe a precipitate that was collected by filtration, exhaustively washed with diethyl ether and dried under vacuum to obtain 170 mg of a yellow solid (42% yield).

EA calcd (%) for C<sub>26</sub>H<sub>18</sub>N<sub>4</sub>O<sub>2</sub> (418): C 74.63, H 4.34, N 13.39, O 7.65; found: C, 73.49; H, 4.28; N, 14.01.

MS-MALDI-TOF (synapinic acid): m/z 419.2 [MH<sup>+</sup>]

<sup>1</sup>H-NMR ([d<sub>6</sub>]-DMSO): 13.02 (s, 2H), 9.21 (m, 4H), 8.98-9.10 (dd, 2H), 8.27 (d, 2H), 7.80-8.06 (m, 2H), 7.51 (t, 2H), 7.10-7.25 (m, 4H).

IR:  $\nu$  (cm<sup>-1</sup>) = 3460 (OH), 3066, 3011, 2981, 2936, 2705 (CH), 1625 (C=N phen), 1514 (C=N imine).

**Synthesis of (3).** **3** was synthesized adapting the procedure described by Pellegrin *et al.*<sup>10</sup> 60 mg (0.12 mmol) of *cis*-Ru(bpy)<sub>2</sub>Cl<sub>2</sub> and 47 mg (0.28 mmol) of AgNO<sub>3</sub> were suspended

in 10 mL of methanol. The mixture was stirred for one hour under inert atmosphere and the white precipitate of AgCl filtered off. 58 mg (0.12 mmol) of **2** dissolved in dichloromethane were added to the clear red solution followed by some drops of triethylorthoformate. The mixture was stirred and heated to reflux overnight under nitrogen. The solvent was removed from the reddish solution, the crude product was redissolved in acetone and an excess of tetra-*n*-butylammonium chloride was added, observing the precipitation of a brown solid. The precipitate was collected and exhaustively washed with diethyl ether to remove the excess of the salt. After removal of the solvent, the solid was purified by using chromatography in neutral alumina with dichloromethane/methanol (95:5) as eluent, the first fraction recovered and the solvent evaporated to obtain 90 mg of an orange solid (66% yield).

EA calcd (%) for C<sub>62</sub>H<sub>66</sub>Cl<sub>2</sub>N<sub>8</sub>O<sub>2</sub>Ru (1126): C 66.06, H 5.90, N 9.94; found: C, 67.02; H, 5.93; N, 10.00.

<sup>1</sup>H-NMR ([d<sub>6</sub>]-DMSO): 12.77 (s, 2H), 9.38 (d, 2H), 9.25-9.35 (dd, 4H), 8.92 (s, 2H), 8.78 (d, 2H), 8.66 (t, 2H), 8.57 (t, 2H), 8.33 (d, 2H), 8.18-8.30 (m, 4H), 8.06-8.12 (m, 2H), 7.81 (t, 4H), 7.62 (t, 2H), 7.38 (m, 4H).

IR:  $\nu$  (cm<sup>-1</sup>) = 3426 (OH), 3064, 2970, 2922, 2857 (CH), 1607 (C=N phen), 1585 (C=N imine).

**Synthesis of [Ru(bpy)<sub>2</sub>CoPhnSlp(Cl)<sub>2</sub>] (1).** To a solution of 50 mg (0.05 mmol) of **3** in 10 mL of methanol was added 13 mg (0.05 mmol) of Co(CH<sub>3</sub>COO)<sub>2</sub>·4H<sub>2</sub>O and stirred overnight at room temperature. Addition of diethyl ether induced precipitation of a solid that was filtered and washed extensively with diethyl ether to obtain 48 mg of an orangish-brown solid (91% yield).

EA calcd (%) for C<sub>46</sub>H<sub>32</sub>Cl<sub>2</sub>CoN<sub>8</sub>O<sub>2</sub>Ru (959): C 57.57, H 3.36, N, 11.68; found: C 57.49, H, 3.50; N, 11.79.

IR:  $\nu$  (cm<sup>-1</sup>) = 3067, 2969, 2923, 2848 (CH), 1607 (C=N phen), 1552 (C=N imine), 553 (Co-O).

**Elemental analysis.** Elemental analysis were performed with a CE Instrument, EA 1110 CHNS.

#### Cyclic Voltammetry

Cyclic voltammeteries were recorded on a BAS EC-epsilon labstation, with a glassy carbon (3 mm diameter) and a Pt wire as working and auxiliary electrodes, respectively. An Ag/AgCl (3 M NaCl) was used as the reference electrode.

#### UV-Vis and emission spectroscopy

UV-Vis absorption spectra were recorded on a UV/Vis/NIR Jasco V-570. Emission spectra were taken on a Horiba-Jobin Yvon Fluoromax-2 spectrofluorimeter, equipped with a Hamamatsu R3896 tube.

**Ultrafast Spectroscopy (UFS).** Femtosecond time-resolved experiments were performed using a pump-probe setup based on the Spectra-Physics Hurricane Ti:sapphire laser source and the Ultrafast Systems Helios spectrometer.<sup>21</sup> The 400-nm pump pulses were generated with a Spectra Physics SHG. Probe pulses were obtained by continuum generation on a sapphire plate (useful spectral range: 450-800 nm). Effective time resolution *ca.* 300 fs, temporal chirp over the white-light 450-750 nm range *ca.* 200 fs, temporal window of the optical delay

stage 0–2000 ps. The time-resolved spectral data were analyzed with the *Ultrafast Systems Surface Explorer Pro* software.

**Nanosecond Laser Flash Photolysis.** Nanosecond transient measurements were performed with a custom laser spectrometer comprised of a *Continuum Surelite II* Nd:YAG laser (FWHM 6–8 ns) with frequency doubled, (532 nm, 330 mJ) or tripled, (355 nm, 160 mJ) option, an *Applied Photophysics* xenon light source including a mod. 720 150 W lamp housing, a mod. 620 power controlled lamp supply and a mod. 03–102 arc lamp pulser. Laser excitation was provided at 90° with respect to the white light probe beam. Light transmitted by the sample was focused onto the entrance slit of a 300 mm focal length *Acton SpectraPro 2300i* triple grating, flat field, double exit monochromator equipped with a photomultiplier detector (*Hamamatsu R3896*) and a *Princeton Instruments PIMAX II* gated intensified CCD camera, using a *RB Gen II* intensifier, a ST133 controller and a PTG pulser. Signals from the photomultiplier (kinetic traces) were processed by means of a *LeCroy 9360* (600 MHz, 5 Gs/s) digital oscilloscope.

#### Photocatalytic water oxidation

Photocatalytic water oxidation tests were conducted in a home-made glass reactor equipped with a steel cap, where a FOXY-R-AF probe was mounted and interfaced with a Neofox Real-Time software for data collection. Irradiation was performed with a monochromatic LED (7 mW power) emitting at 450 nm; the photon flux was  $2.63 \times 10^{-8}$  einstein/s.

#### Acknowledgements

This work was supported by the Italian MIUR (FIRB “NanoSolar” RBAP11C58Y, PRIN “Hi-Phuture” 2010N3T9M4\_001) and by Fondazione Cariparo (Nanomode, progetti di eccellenza 2010). COST Actions CM1003 “Biological oxidation reactions - mechanisms and design of new catalysts” and CM1203 “Catalytic Routines for Small Molecule Activation (CARISMA)” are gratefully acknowledged.

#### Notes and references

<sup>a</sup> ITM-CNR and Department of Chemical Sciences, University of Padova, via Marzolo 1, 35131 Padova, Italy.

<sup>b</sup> Department of Chemical and Pharmaceutical Sciences, University of Ferrara, and Centro Interuniversitario per la Conversione Chimica dell’Energia Solare (sez. Ferrara), via Fossato di Mortara 17–19, 44121 Ferrara, Italy.

<sup>c</sup> ISOF-CNR c/o Department of Chemical and Pharmaceutical Sciences, University of Ferrara, Via Luigi Borsari 46, 44121 Ferrara, Italy

¥ These authors contributed equally to the paper.

♣ In some cases, oxidation of a salophen moiety with a transition metal inserted can still occur, through the formation and stabilisation of radical derivatives.<sup>22</sup>

\*\* Complete quenching of the emission was also found for a very similar compound,<sup>10a</sup> though in that case the mechanism was thought to be oxidative quenching of the ruthenium sensitizer and reduction of the salophen moiety.

† In the forward step of an oxidative quenching process, conversion of the \*Ru(II) MLCT state into the Ru(III) oxidized form is expected to essentially maintain the MLCT bleach at 450 nm. The spectral changes expected upon generation of a Co(I) species are difficult to predict, as no reliable solution spectrum for such a species is available.<sup>13,14b</sup> They are presumably small in this spectral region, dominated by the ruthenium polypyridine chromophore.<sup>9</sup>

§ A similar recovery in emission intensity is obtained with **3** in acetonitrile upon addition of HClO<sub>4</sub>.

¶ The CV scan in aqueous phosphate buffer, pH 7 (figure S6 in ESI), does not support complete Co release from **1** with formation of **3**; in fact the CV of **1** is clearly different, lacking the irreversible waves due to oxidation of the phenolic groups (at 0.7 and 1.05 V in **3**) and with an additional catalytic wave due to water oxidation starting at E = 1.05 V.

♦ It is generally assumed that aqueous Co(II) evolves to Cobalt oxide nanoparticles under water oxidation conditions. The spent reaction mixture, collected after oxygen evolution by **1**, has thus been analysed by dynamic light scattering (DLS) to get insight into the presence of colloidal Cobalt oxides. These experiments however were not conclusive, since the scattering intensity was found to be close to the detection limit of the instrument.

◇ A very similar process, electron transfer from the phenolic groups to the ruthenium center of the MLCT excited state, is observed to take place in 45 ps in the ultrafast spectroscopy of **3** in acetonitrile (Figure 5a). The hole transfer process envisioned here, with a greater driving force, is expected to be at least as fast.

Electronic Supplementary Information (ESI) available: <sup>1</sup>H-NMR of **2** and **3**, kinetic analysis obtained by UFS on **1** and **3**, laser flash photolysis on **3**, electrochemistry of **1** and **3** in aqueous buffer. See DOI: 10.1039/b000000x/

- Faraday Disc.*, 2012, **155**, 1–388 themed issue Artificial Photosynthesis.
- (a) J. H. Alstrum-Acevedo, M. K. Brennaman and T. J. Meyer, *Inorg. Chem.*, 2005, **44**, 6802. (b) V. Balzani, A. Credi and M. Venturi, *ChemSuschem*, 2008, **1**, 26.
- (a) A. R. Parent, R. H. Crabtree and G. W. Brudvig, *Chem. Soc. Rev.* 2013, **42**, 2247. (b) A. Singh and L. Spiccia, *Coord. Chem. Rev.*, 2013, **257**, 2607. (c) A. Sartorel, M. Bonchio, S. Campagna and F. Scandola, *Chem. Soc. Rev.*, 2013, **42**, 2262.
- (a) A. Sartorel, M. Carraro, F. M. Toma, M. Prato and M. Bonchio, *En. Env. Sci.*, 2012, **5**, 5592. (b) K. J. Young, L. A. Martini, R. L. Milot, R. C. Snoeberger, V. S. Batista, C. A. Schmuttenmaer, R. H. Crabtree and G. W. Brudvig, *Coord. Chem. Rev.*, 2012, **256**, 2503. (c) F. Puntoriero, A. Sartorel, M. Orlandi, G. La Ganga, S. Serroni, M. Bonchio, F. Scandola and S. Campagna, *Coord. Chem. Rev.*, 2011, **255**, 2594.
- H.S. White, W.G. Becker and A. J. Bard, *J. Phys. Chem.*, 1984, **88**, 1840.
- (a) Y. Gao, X. Ding, J. Liu, L. Wang, Z. Lu, L. Li, L. Sun, *J. Am. Chem. Soc.*, 2013, **135**, 4219. (b) M. Orlandi, R. Argazzi, A. Sartorel, M. Carraro, G. Scorrano, M. Bonchio, F. Scandola, *Chem. Commun.*, 2010, **46**, 3152. (c) X. Xiang, J. Fielden, W. RodríguezCórdoba, Z. Huang, N. Zhang, Z. Luo, D. Musaev, T. Lian, C. L. Hill, J. *Phys. Chem. C*, 2013, **117**, 918. (d) W. Youngblood, S. Lee, Y.



- Kobayashi, E. Hernandez Pagan, P. Hoertz, T. Moore, A. Moore, D. Gust, T. Mallouk, *J. Am. Chem. Soc.*, 2009, **131**, 926. (e) Y. Zhao, J. R. Swierk, J. D. Megiatio, B. Sherman, W. J. Youngblood, D. Qin, D. M. Lentz, A. L. Moore, T. A. Moore, D. Gust and T. A. Mallouk, *Proc. Nat. Acad. Sci. U.S.A.*, 2012, **39**, 15612.
- 7 (a) P. G. Hoertz, Y.-I. Kim, J. Youngblood and T. E. Mallouk, *J. Phys. Chem. B*, 2007, **111**, 6845. (b) N. Morris, M. Suzuki, T. Mallouk, *J. Phys. Chem. A*, 2004, **108**, 9115. (c) M. Hara, C. C. Waraksa, J. T. Lean, B. A. Lewis and T. E. Mallouk, *J. Phys. Chem. A*, 2000, **104**, 5275. (d) F. Puntoriero, G. La Ganga, A. Sartorel, M. Carraro, G. Scorrano, M. Bonchio and S. Campagna, *Chem. Commun.*, 2010, **46**, 4725. (e) S. Berardi, G. La Ganga, M. Natali, I. Bazzan, F. Puntoriero, A. Sartorel, F. Scandola, S. Campagna and M. Bonchio, *J. Am. Chem. Soc.*, 2012, **134**, 11104. (f) G. La Ganga, F. Puntoriero, S. Campagna, I. Bazzan, S. Berardi, M. Bonchio, A. Sartorel, M. Natali and F. Scandola, *Faraday Disc.*, 2012, **155**, 177. (g) M. Natali, M. Orlandi, S. Berardi, S. Campagna, M. Bonchio, A. Sartorel and F. Scandola *Inorg. Chem.* 2012, **51**, 7324. (h) M. Natali, S. Berardi, A. Sartorel, M. Bonchio, S. Campagna and F. Scandola *Chem. Commun.* 2012, **48**, 8808.
- 8 (a) L. Sun, H. Berglund, R. Davydov, T. Norrby, L. Hammarström, P. Korall, A. Börje, C. Philouze, K. Berg, A. Tran, M. Andersson and G. Stenhagen, J. Mårtensson, M. Almgren, S. Styring and B. Åkermark, *J. Am. Chem. Soc.* 1997, **119**, 6996. (b) L. Sun, M. K. Raymond, A. Magnuson, D. Le Gourrière, M. Tamm, M. Abrahamsson, P. Huang Kenéz, J. Mårtensson, G. Stenhagen, L. Hammarström, S. Styring and B. Åkermark, *J. Inorg. Biochem.*, 2000, **78**, 15. (c) K. Berg, A. Tran, M. Raymond, M. Abrahamsson, J. Wolny, S. Redon, M. Andersson, L. Sun, S. Styring, L. Hammarström, H. Toftlund and B. Åkermark, *Eur. J. Inorg. Chem.*, 2001, 1019. (d) L. Sun, M. Abrahamsson, H. Baudi, S. Styring and L. Hammarström, *Inorg. Chem.*, 2002, **41**, 1534. (e) A. Johansson, M. Abrahamsson, A. Magnuson, P. Huang, J. Mårtensson, S. Styring, L. Hammarström, L. Sun and B. Åkermark, *Inorg. Chem.*, 2003, **42**, 7502. (f) R. Lomoth, P. Huang, J. Zheng, L. Sun, L. Hammarström, B. Åkermark and S. Styring, *Eur. J. Inorg. Chem.* 2002, 2965. (g) D. Burdinski, K. Wiegardt and S. Steenken, *J. Am. Chem. Soc.*, 1999, **121**, 10781. (h) D. Burdinski, E. Bothe and K. Wiegardt, *J. Am. Chem. Soc.*, 2000, **39**, 105. (i) L. Sun, M. Burkitt, M. Tamm, M. Raymond, M. Abrahamsson, D. Legourrière, Y. Frapart, A. Magnuson, P. Kenéz, P. Brandt, A. Tran, L. Hammarström, S. Styring and B. Åkermark, *J. Am. Chem. Soc.*, 1999, **121**, 6834. (l) M. Sjödin, S. Styring, B. Åkermark, L. Sun and L. Hammarström, *J. Am. Chem. Soc.*, 2000, **122**, 3932. (m) Y. Xu, G. Eilers, M. Borgström, J. Pan, M. Abrahamsson, A. Magnuson, R. Lomoth, J. Bergquist, T. Polívka, L. Sun, V. Sundström, S. Styring, L. Hammarström and B. Åkermark, *Chem. Eur. J.*, 2005, **11**, 7305. (n) P. Farràs, S. Maji, J. Beneta Buchholz and A. Llobet, *Chem. Eur. J.*, 2013, **19**, 7162. (o) F. Li, Y. Jiang, B. Zhang, F. Huang, Y. Gao and L. Sun, *Angew. Chem. Int.*, 2012, **51**, 2417. (p) K. Hanson, D. Torelli, A. Vannucci, M. Brennaman, H. Luo, L. Alibabaei, W. Song, D. Ashford, M. Norris, C. Glasson, J. Concepcion and T. J. Meyer, *Angew. Chem. Int. Ed.*, 2012, **51**, 12782.
- 9 E. Pizzolato, M. Natali, B. Posocco, A. Montellano López, I. Bazzan, M. Di Valentin, P. Galloni, V. Conte, M. Bonchio, F. Scandola and A. Sartorel, *Chem. Commun.*, 2013, **49**, 9941.
- 10 (a) Y. Pellegrin, A. Quaranta, P. Dorlet, M. F. Charlot, W. Liebl and A. Aukauloo, *Chem. Eur. J.*, 2005, **11**, 3698. (b) Y. Pellegrin, K. E. Berg, G. Blondin, E. Anxolabéhère-Malart, W. Leibl and A. Aukauloo, *Eur. J. Inorg. Chem.*, 2003, 1900.
- 11 (a) M. Yamada, Y. Tanaka, Y. Yoshimoto, S. Kuroda and I. Shimao *Bull. Chem. Soc. Jpn.*, 1992, **65**, 1006. (b) S. Bodge and F. M. MacDonnell, *Tetrahedron Letters*, 1997, **38**, 8159.
- 12 C. V. Krishnan, C. Creutz, H. A. Schwarz and N. Sutin *J. Am. Chem. Soc.* 1983, **105**, 5617-5623.
- 13 A. A. Isse, A. Gennaro, E. Vianello, and C. Floriani, *J. Mol. Catal.*, 1991, **70**, 197.
- 14 (a) A. Pui, C. Dobrota and J. P. Mahy, *J. Coord. Chem.*, 2007, **60**, 581. (b) B. Ortiz and S. M. Park, *Bull. Korean Chem. Soc.*, 2000, **21**, 405. (c) N. B. Pahor, M. Calligaris, P. Delise, G. Dodic, G. Nardin and L. Randaccio, *J. Chem. Soc., Dalton Trans.*, 1976, 2478. (d) B. J. Kennedy, G. D. Fallon, B. M. K. C. Gatehouse and K. S. Murray, *Inorg. Chem.* 1984, **23**, 580.
- 15 (a) S. Campagna, F. Puntoriero, F. Nastasi, G. Bergamini and V. Balzani, *Top. Curr. Chem.*, 2007, **280**, 117 and references therein. (b) M. N. Achermann and L. V. Interrante, *Inorg. Chem.*, 1984, **23**, 3904.
- 16 L. A. Kelly and M. A. J. Rodgers, *J. Phys. Chem.*, 1994, **98**, 6377.
- 17 (a) S. H. Alarcón, D. Pagani, J. Bacigalupo and A. C. Olivieri, *J. Mol. Struct.*, 1999, **475**, 233. (b) P. M. Dominiak, E. Grech, G. Barr, S. Teat, P. Mallinson and K. Woźniak, *Chem. Eur. J.*, 2003, **9**, 963.
- 18 A. A. Khandar, B. Shaabani, F. Belaj, A. Bakhtiari *Inorg. Chim. Acta* 2007, **360**, 3255
- 19 (a) D. Hong, J. Jung, Y. Yamada, T. Suenobu, Y.-M Lee, W. Nam and S. Fukuzumi *En. Env. Sci.* 2012, **5**, 7606. (b) D. Wang and T. J. Groves *Proc. Nat. Acad. Sci. U.S.A.* 2013, **110**, 15579.
- 20 T. A. Heimer, E. J. Heilweil, C. A. Bignozzi and G. J. Meyer, *J. Phys. Chem. A*, 2000, **104**, 4256.
- 21 C. Chiorboli, M. A. J. Rodgers and F. Scandola, *J. Am. Chem. Soc.*, 2003, **125**, 483.
- 22 (a) A. Kochem, O. Jarjays, B. Baptiste, C. Philouze, H. Vezin, K. Tsukidate, F. Tani, M. Orio, Y. Shimazaki and F. Thomas, *Chem. Eur. J.*, 2012, **18**, 1068. (b) D. de Bellefeuille, M. S. Askari, B. Lassalle-Kaiser, Y. Journaux, A. Aukauloo, M. Orio, F. Thomas and X. Ottenwaelder, *Inorg. Chem.*, 2012, **51**, 12796.